Journal of Civil Engineering and Architecture 20 (2026) 417-436
doi: 10.17265/1934-7359/2026.10.001

Machine Recognition of Elastoplastic Materials in Material Genetics

P. A. Belov[1], N. Ya. Golovina[2] and Elliot Weiss[3]

1. Institute of Applied Mechanics of the Russian Academy of Sciences, Moscow 125040, Russia

2. Industrial University of Tyumen (IUT), Surgut Branch, Surgut 628400, Tyumen Region, Russia

3. Independent Researcher, USA

Abstract: The studies [12, 13] separated two levels of material identification: Geometry Builder determines the morphology and the local $C^0/C^1/C^2$ class structure of the deformation curve, whereas Material Builder solves the first physical inverse problem for a fixed architecture. The present work combines these levels into a machine-recognition problem in which the architecture and the observable physical passport are mutually dependent variables. The main theoretical result is a finite-dimensional reduction of the physically generalized Reinsch principle for an irreversible material. After the solution is represented in the genetic basis, the reversible integrals and antisymmetric Pfaffian channels are analytically integrated with respect to strain and condensed into segment matrices. The resulting target form is analogous to the Ritz method in its finite-dimensional reduction mechanism, but differs in the underlying principle: stationarity of a nonintegrable variational Pfaffian form is required instead of stationarity of potential energy. At each step of the deterministic genealogy, the point of maximum absolute defect specifies the reproduction location, while the profiled Ritz-Reinsch form selects the physically preferable admissible pair of offspring classes after closure of the observable Material Passport. For a prescribed experimental resolution δ, the recognition result is the first genealogical state satisfying $E_{RMS} \le \delta$ and $E_{\infty} \le \delta$. The resulting model is therefore not claimed to be the global minimum among all conceivable partitions; it is the least-complex experimentally admissible state of the deterministic Recognition genealogy.

Key words: Material genetics, machine recognition, morphology, model architecture, first inverse problem, approximation spline, Material Passport, generalized Reinsch principle, Pfaffian form, design of experiments, Geometry Builder, Material Builder.

1. Introduction

Machine recognition of an elastoplastic material starts from a finite experimental sample $D = \{(\varepsilon_k, \sigma_k)\}_{k=1}^{N}$. The first natural task is to construct a continuous stress-strain relation consistent with the measurements. The classical least-squares method, originating with Legendre [1], addresses precisely this task: among the functions of a prescribed family, it selects the one for which the mean squared residual is minimal,

$$\theta^* = \arg\min_{\theta} \frac{1}{N} \sum_{k=1}^{N} w_k \left[\sigma_k - \hat{\sigma}(\varepsilon_k; \theta)\right]^2 \qquad (1)$$

Equation (1) answers how accurately a prescribed family of functions reproduces the sample, but it does not answer the prior question of which family should be chosen. Attempting to remove this ambiguity by global interpolation, i.e., by requiring a single function to pass exactly through all experimental points, creates a new problem. Runge [2] showed that increasing the number of nodes and the degree of the interpolation polynomial does not by itself guarantee improved behavior between the nodes. The classical example

$$f(x) = \frac{1}{1 + 25x^2}, \qquad -1 \le x \le 1, \qquad (2)$$

demonstrates the growth of endpoint oscillations of interpolation polynomials at equally spaced nodes. Thus, accuracy at the nodes alone is insufficient; the behavior of the function between observations must

Corresponding author: Petr A. Belov, D.Sc. (Phys.-Math.), Leading Researcher, research fields: mechanics of materials, constitutive modeling, inverse problems, materials genetics.

also be controlled.

This leads to the next task: introducing a measure of regularity of the sought function. The functional-analytic framework of Sobolev [3] makes it possible to formulate this requirement through joint control of the function and its generalized derivatives. In the one-dimensional case, the space

$$W_2^m(a,b) = \{u:\ u, u', \dots, u^{(m)} \in L_2(a,b)\},$$

$$\| u \|^2_{W_2^m} = \sum_{j=0}^{m} \int_a^b \left|u^{(j)}(x)\right|^2 dx. \tag{3}$$

The Sobolev formulation provides a language in which smoothness becomes measurable, but it does not yet specify how smoothness should be reconciled with a finite experimental sample. This next step was realized in smoothing-spline theory, prepared by the work of Schoenberg [4] and brought to a computationally complete form by Reinsch [5]. In the classical Reinsch formulation, a function of minimum curvature is selected subject to an admissible residual level,

$$\min_s \int_a^b \left[s''(x)\right]^2 dx,$$

$$\sum_{k=1}^{N} \left[\frac{y_k - s(x_k)}{\delta y_k}\right]^2 \le S. \tag{4}$$

The equivalent Lagrangian form reveals the mechanism of the trade-off between data fidelity and smoothness,

$$J_R[s] = \sum_{k=1}^{N} w_k \left[y_k - s(x_k)\right]^2 + \lambda \int_a^b [s''(x)]^2 \, dx \to \min. \tag{5}$$

Reinsch thus resolves the problem exposed by Runge: accuracy at the nodes ceases to be the sole criterion. A physical problem, however, then arises. A subjectively selected coefficient λ controls mathematical smoothness but is not a material characteristic; moreover, a single global curvature measure does not explain why different portions of a deformation curve may possess different local structures. Material recognition therefore requires simultaneous determination of both the partition of the curve into segments and the physical law on each segment.

The classical sequence is explicit in the least-squares residual (1), the Runge interpolation example (2), the Sobolev regularity setting (3), and the constrained and Lagrangian Reinsch formulations (4)-(5).

In parallel, statistics developed another route to model selection—DoE (Design of Experiment), systematically developed by Fisher [6]. Classical DoE organizes variation of preselected factors and levels so that their influence on the response can be assessed from a finite number of experiments and a preferable region of factor space can be selected. DoE itself, however, presupposes that the factor set, model parameterization, and optimality criterion have already been specified. In material recognition, not only the passport parameters but also the model architecture is unknown. In the present work, the DoE idea is therefore transferred to a deterministic genealogy of information-admissible models: the geometric direction is prescribed by the maximum absolute defect, the profiled Ritz-Reinsch form ranks local class variants, and the first state reaching the prescribed experimental resolution terminates the search.

A constructive prototype for the first part of this problem is provided by an algorithm opposite in direction to the Douglas-Peucker algorithm [7]. For a fragment of a discrete curve between points P_i and P_j, the point with the maximum deviation from the chord joining them is selected,

$$k^* = \arg\max_{i<k<j} d\left(P_k, \overline{P_i P_j}\right). \tag{6}$$

If this maximum deviation exceeds the prescribed tolerance, the selected point becomes the division point of the original fragment. Local geometric inhomogeneity therefore generates the segmentation itself. The Douglas-Peucker algorithm remains purely geometric, however: it does not determine the smoothness class of the resulting segments and does not relate their boundaries to the physical properties of the material.

Equation (6) specifies the geometric maximum-deviation prototype used in the subsequent construction.

This is where the concepts used below become necessary. Morphology is defined as the segmented structure of the experimental deformation curve and comprises the number of segments and the ordered coordinates of their internal boundaries. Architecture is defined as the morphology supplemented by the local smoothness class, C^0, C^1, or C^2, assigned to each segment. Thus, morphology answers the question "where are the segment boundaries?", whereas architecture additionally answers "to which differential class does each segment belong?". The distribution of experimental points among the segments is uniquely induced by the selected boundaries and therefore is not an independent component of the definition of morphology.

The physical content of this geometric structure is supplied by the concept of material genetics developed in [8–11]. It is not a biological hypothesis but a mathematical structural analogy: a material is described by an initial differential operator, and factorization of that operator defines a hierarchy of its elementary constituents. The genotype is the finite-dimensional functional space of fundamental solutions of the initial operator; an allele is a second-order operator in its factorization; a gene is a first-order operator together with the corresponding fundamental solution; and the phenotype is the set of coefficients in the expansion of stress in the space of fundamental solutions (genes) [8-10]. These definitions are not introduced as a terminological metaphor; they transfer the choice of an approximating function from an arbitrary family to a family of solutions of a physically defined operator.

The primary physical object of material genetics is not potential energy itself but a nonintegrable variational 1-form. For the derivative vector $q_i = d^i\sigma/d\varepsilon^i$, its reversible and irreversible parts are specified by the symmetric tensor A and the antisymmetric tensor B:

$$\delta\mathcal{W} = \delta\left(J_D + \int_{\varepsilon_a}^{\varepsilon_b}\sum_{i,j} A_{ij}\, q_i q_j\, d\varepsilon\right) + \int_{\varepsilon_a}^{\varepsilon_b}\sum_{i,j} B_{ij}\left(q_i\,\delta q_j - q_j\,\delta q_i\right)d\varepsilon = 0, \quad A_{ij} = A_{ji}, \quad B_{ij} = -B_{ji}. \tag{7}$$

Stationarity of the variational 1-form (7) generates the Euler equation and natural boundary conditions; factorization of the resulting operator determines its alleles, genes, and characteristic roots [8-10]. Reinsch regularization therefore acquires a physical interpretation: the integral measure of derivatives can be replaced by a quadratic form of reversible properties A, whereas irreversible properties enter through oriented channels of the 1-form B, rather than through an artificial scalar smoothness coefficient.

Accordingly, the material variational 1-form (7) supplies the physical regularization mechanism, while the joint recognition problem (8) couples architecture and the observable Material Passport.

This formulation successively generated two partial problems. The study [12] addressed the geometric problem: morphology and architecture—the segment boundaries and their classes C^0 / C^1 / C^2 —were determined from a finite sample. The arbitrariness of a global partition was thereby removed, but the physical passport was not a variable of the morphological search. The study [13] addressed the next problem: for an already fixed architecture, a physically regularized approximation spline was constructed and the first physical inverse problem was solved. In that case the physics varied, whereas segment boundaries and classes were prescribed. In the present work, the deterministic boundary-location genealogy of [12] is retained, whereas its structural assignment of offspring classes is not inherited unchanged: the offspring classes become local alternatives that are compared only after the fixed-architecture physical closure of [13].

In the present work, the Material Passport is

understood as a single traceable set of parameters linking the observed curve to the operator that generated it. It contains two subsets. The first is the observable operator passport of the first inverse problem: the characteristic roots and two coefficient combinations entering the natural boundary conditions. The second is the full physical passport: the components of the symmetric tensor A and antisymmetric tensor B, related to the characteristic roots through the coefficients of the characteristic polynomial and Vieta relations. The first inverse problem directly identifies the first subset; the second subset, i.e., the full physical passport, must not be artificially declared a direct output of the first inverse problem.

Comparison of the results in [12] and [13] reveals the remaining problem. An architecture found without simultaneous physical identification may change once the physical regularizer is taken into account; conversely, a physical passport identified on a preassigned architecture depends on that architecture. Hence the sequential scheme "geometry first, physics second" does not ensure self-consistency of the "architecture-material passport" pair. This dependence gives rise to the problem addressed in the present work.

Let Γ denote the architecture and χ the observable physical passport. Instead of two sequential problems, we therefore formulate a single joint variational problem.

Here and below, "joint recognition" does not mean simultaneous free minimization over architecture and over the components of the complete physical tensors A and B. The problem has a nested structure. For every admissible candidate architecture Γ, Material Builder first solves the first physical inverse problem with Γ fixed and closes only the observable passport χΓ*. Recognition then compares the resulting physically closed architectural candidates through the profiled form $\int_R$ (Γ,χΓ*). Thus, architecture is an external discrete variable of the deterministic genealogy, whereas the observable Material Passport is the internal solution of the first inverse problem for a fixed architecture. No independent variation of the underdetermined components of the complete A/B passport is introduced.

$$(\Gamma^*, \chi^*) = \underset{\Gamma \in \mathfrak{A}_N,\ \chi \in \mathfrak{X}}{\arg\min}\, \mathcal{R}(\Gamma, \chi), \tag{8}$$

where $\mathfrak{A}_N$ is the finite set of information-admissible architectures, $\mathfrak{X}$ is the admissible space of observable passports, and $\mathcal{R}$ is the physically generalized Reinsch functional (7). Its discrete part J_D measures agreement with the experimental sample, the reversible integral part is determined by the symmetric tensor A, and the irreversible part by dissipation channels represented as 1-forms defined by the antisymmetric tensor B. The number and classes of segments enter the functional through actual segment contributions and the information-admissibility condition, not through an artificial complexity penalty.

The position of the present work in this development is therefore determined not by a mere list of preceding methods, but by the successive removal of their limitations. Least squares provide agreement with the sample but require a preselected function family; the Runge phenomenon demonstrates the inadequacy of exact global interpolation; Sobolev spaces introduce measurable regularity; the Reinsch approach couples regularity to residual error but uses a nonphysical, subjectively selected smoothness parameter λ; Fisher's DoE [6] provides a systematic response-based selection framework in a prescribed factor space but does not solve the simultaneous selection of the physical model architecture itself; the inverse counterpart of the Douglas-Peucker approach shows how geometric inhomogeneity generates segmentation but does not determine its physics; material genetics relates the curve shape to a differential operator and a physical 1-form; [12] determines the architecture without simultaneous physical identification; and [13] identifies the physics for a fixed architecture. The mutual dependence of architecture and material passport created by the last two limitations is removed here by their joint variational identification.

Statement 2 (gauge-invariant closure of the observable passport). For a fixed admissible architecture, the observable projection of the Material Passport is uniquely specified by: (i) the characteristic roots determined by the genes; and (ii) the active boundary combinations g₀ and g_1 determined by the stationary natural conditions of the target Ritz-Reinsch 1-form. After quotienting out the exact-derivative A_{13} / B_{13} directions, the value of the observable form $\hat{J}_R$ is independent of the component representative chosen for the full A/B passport.

Proof. A shift of A_{13} accompanied by the consistent shift of A_{22} leaves the combination ($2A_{13}$-A_{22})/A_{33} unchanged and alters the reversible integral contribution only by an exact boundary derivative; B_{13} likewise enters only through an exact boundary derivative of the dissipative channel. After these directions are factored out, the bulk form depends on the coefficients $a_0, \dots, a_3$, uniquely determined by the roots through Vieta relations, and on the observable natural-boundary combinations. The latter are not selected arbitrarily: their values are determined by setting the corresponding boundary coefficients of the first variation to zero. Consequently, two full A/B representatives having the same gene roots and the same stationary observable boundary combinations yield the same value of $\hat{J}_R$.

The purpose of the present work is to formulate and investigate this joint problem, derive the reversible and irreversible parts of the physically generalized Reinsch principle in the gene representation, construct a finite architecture-search algorithm with a constructive stopping condition, define the two-level structure of the Material Passport, and implement the resulting scheme in the Recognition computational utility.

2. Problem Formulation: Joint Recognition of Architecture and the Physical Passport

The studies [12] and [13] define two mutually complementary sections of a single problem. In [12], construction of morphology determines the segment boundaries and, together with the assigned local C^0 / C^1 / C^2 classes, defines the architecture of the deformation curve, whereas the physical description is not a search variable. In [13], by contrast, the architecture is fixed and the first inverse problem determines the observable operator passport of the physical model. In the present work both restrictions are removed. The recognition object is the self-consistent "architecture-physical passport" pair.

Let the experimental sample be given by the ordered set

$$D = \{(\varepsilon_k, \sigma_k)\}_{k=1}^{N}.$$

We denote the morphology by

$$\Gamma = \{m_0, m_1, m_2;\ q_1, \dots, q_m;\ \varepsilon_1, \dots, \varepsilon_{m-1}\},$$

A segment of class C^q is called information-admissible if the portion of the experimental sample belonging to it contains at least $n_q = 2(q+1)$ distinct points, i.e., at least 2 points for C^0, 4 points for C^1, and 6 points for C^2. This is the minimum amount of data required to determine the n_q phenotype coefficients of a segment of that class. An architecture is information-admissible if each of its segments is information-admissible. Because adjacent segments share a boundary point, an architecture with m_0, m_1, and m_2 segments of classes C^0, C^1, and C^2, respectively, requires at least $m_0 + 3m_1 + 5m_2 + 1$ distinct sample points; this condition defines the finite set of admissible architectures below.

Here $q_s \in \{0,1,2\}$ denotes the segment smoothness class, m_q is the number of segments of class C^q, and $m = m_0 + m_1 + m_2$ is the total number of segments. For a prescribed number N of sample points, the admissible segment counts belong to the finite set

$$\mathcal{M}_N = \{(m_0, m_1, m_2) \in \mathbb{N}_0^3 :\ m_0 + 3m_1 + 5m_2 + 1 \le N\}.$$

The corresponding architecture space can conveniently be represented as the disjoint union

$$\mathfrak{A}_N = \bigsqcup_{\mathbf{m} \in \mathcal{M}_N} \mathfrak{A}_{\mathbf{m}}.$$

Let X_r = (Γ_r,χ_r*) be the sequence of self-consistent states of the deterministic Recognition genealogy

generated by reproduction at the point of maximum absolute defect and by local selection of offspring classes according to the profiled form $\int_R$. For a prescribed experimental resolution δ, the general problem of the present work is

$$r* = min\{r: E_RMS(X_r) \le \delta \wedge E_\infty(X_r) \le \delta\}, X*(\delta) = X_r* \quad (9a)$$

Equation (9a) defines the first experimentally admissible state specifically on the constructed deterministic genealogy. The physical passport of each X_r is first closed for the fixed architecture, and the local offspring classes are selected according to $\int_R$. Thus, Equation (9a) is not a global minimization over the set of all possible architectures.

The geometric part of the genealogy inherits from [12] only the deterministic geometric reproduction rule: for a fixed physical interpretation, the next boundary is uniquely specified by the point of the global maximum absolute residual, and all previously accepted boundaries are retained. The inheritance from [12] is deliberately restricted to this geometric rule. The rule for assigning local classes to the offspring is not inherited unchanged. In [12], class assignment belongs to the structural construction itself, whereas in the present Recognition problem the classes of the two offspring constitute local discrete alternatives. Each admissible pair is subjected to the fixed-architecture physical closure of [13], and the profiled Ritz-Reinsch form $\int_R$ selects the physically preferable pair. Thus, the present work preserves the deterministic geometric genealogy of [12] while replacing its purely structural class assignment by a physically relaxed local class selection.

For a fixed architecture, the first physical inverse problem of [13] remains the closure of the observable Material Passport for the prescribed segment boundaries and classes.

$$\chi^* = \arg\min_{\chi \in \mathfrak{X}} J(\Gamma_0, \chi). \quad (9b)$$

Thus, the studies [12] and [13] are two coordinate sections of the general problem (9a). The present work removes both restrictions and constructs a deterministic genealogy of self-consistent "architecture-physical passport" pairs. For a prescribed δ, the first experimentally admissible state of this genealogy is selected; no global optimization over all possible partitions is formulated.

The stopping rule (9a) and the fixed-architecture physical closure (9b) therefore form the two coupled levels of the genealogical recognition problem.

3. Generalization of the Reinsch Principle for Reversible Processes

The classical Reinsch principle (5) combines the data residual with a measure of smoothness of the approximating function. In the genetics of materials, the regularizer must not be introduced through an external smoothing coefficient λ: its physical content is specified by the reversible part of the Material Passport. Therefore, in the present work the smoothness term is replaced by a quadratic form of derivatives consistent with the reversible part of functional (7), defined by the symmetric tensor of reversible properties $A = A^T > 0$.

For segment s of class C^q on the interval $\Omega_s = [\varepsilon_{s-1}, \varepsilon_s]$, introduce the integrals

$$I_{ij}^{(s)} = \int_{\varepsilon_{s-1}}^{\varepsilon_s} \sigma_s^{(i)}(\varepsilon)\sigma_s^{(j)}(\varepsilon)\, d\varepsilon, \quad i,j = 1, \dots, q+1. \quad (10)$$

The reversible contribution of a segment is

$$\Pi_s^{(q)} = \frac{1}{2}\sum_{i,j=1}^{q+1} A_{ij}^{(q)} I_{ij}^{(s)}. \quad (11)$$

For the highest class C^2, six independent integrals $I_{11}, I_{12}, I_{13}, I_{22}, I_{23}, I_{33}$ are retained; for C^1, the integrals I_{11}, I_{12}, I_{22}; and for C^0, only I_{11}. This nesting coincides with the nesting of the physical classes in [13].

Introduce the morphological tensor

$$M_{ij} = \sum_{\substack{s \\ q_s+1 \ge \max(i,j)}} I_{ij}^{(s)}, \quad M_{ij} = M_{ji}. \quad (12)$$

Then the total reversible part takes the compact form

$$\Pi_{\mathrm{rev}} = \frac{1}{2}\sum_{i,j} A_{ij}\, M_{ij} \qquad (13)$$

This equality does not imply independence of morphology and physics. On the contrary, $\mathbf{M} = \mathbf{M}(\Gamma, \chi)$, because the fundamental genes and phenotype coefficients depend on the characteristic roots included in the passport. The discrete part J_D of functional (7) contains the residuals between the experimental sample points σ_k and the sought deformation curve $\sigma(\varepsilon_k; \Gamma, \chi)$:

$$J_D(\Gamma, \chi) = \sum_{k=1}^{N} w_k\, [\sigma_k - \sigma(\varepsilon_k; \Gamma, \chi)]^2. \qquad (14)$$

The reversible functional of the generalized Reinsch principle is then defined naturally, without an artificial penalty on the number of segments:

$$J_{\mathrm{rev}}(\Gamma, \chi) = J_D(\Gamma, \chi) + \Pi_{\mathrm{rev}}(\Gamma, \chi). \qquad (15)$$

For a fixed set of segment counts, the internal geometric variables can be eliminated:

$$\mathcal{F}_{\mathrm{rev}}(m_0, m_1, m_2; \chi) = \min_{\Gamma \in \mathfrak{A}_{\mathbf{m}}} J_{\mathrm{rev}}(\Gamma, \chi). \qquad (16)$$

For each admissible candidate architecture, the continuous observable passport coordinates are first eliminated by solving the fixed-architecture first inverse problem. The resulting profiled form is therefore evaluated only after physical closure of that candidate. Recognition acts on these physically closed candidates along the deterministic genealogy; it does not perform an unconstrained simultaneous minimization over architecture and the components of the complete physical passport.

The construction proceeds from the segment derivative integrals (10) and reversible segment contribution (11) to the morphological tensor (12) and its total contraction (13); the data misfit (14) then enters the generalized Reinsch functional (15), whose internal geometric variables are eliminated by profiling in (16).

4. Genetic Representation of a Segment and Analytical Evaluation of the Reversible Form

On a segment of class C^q, the solution is written in the genetic basis

$$\sigma_s(\varepsilon) = \sum_{\alpha=1}^{n_q} f_{s\alpha}\,(\chi)\, g_\alpha^{(q)}(\varepsilon; \chi), \qquad (17)$$

$$n_0 = 2,\ n_1 = 4,\ n_2 = 6.$$

Here s is the segment number; q ∈ {0,1,2} is the order of its smoothness class C^q; n_q = 2(q + 1) is the dimension of the genetic basis of class C^q; α is the gene number in this basis; g_α ^ (q) is the fundamental genetic solution of class C^q; $f_{s\alpha}$ is the corresponding phenotype coefficient of segment s; and χ is the vector of coordinates of the observable physical passport.

The segment index belongs to the phenotype coefficients $f_{s\alpha}$, but not to the fundamental genes: the genes are common to all segments of the same physical class. For the local coordinate $x = \varepsilon - \varepsilon_{s-1},\ 0 \le x \le h_s$, the coefficients are determined by the boundary kinematics of the segment:

$$\mathbf{C}^{(q)}(h_s, \chi)\mathbf{f}_s = \mathbf{d}_s^{(q)},$$
$$\mathbf{f}_s = \left[\mathbf{C}^{(q)}\right]^{-1}\mathbf{d}_s^{(q)}. \qquad (18)$$

In (18), $f_s = (f_{s1}, \dots, f_{sn_q})^T$ is the vector of phenotype coefficients; h_s = ε_s - ε_{s-1} is the length of segment s; $C^{(q)}(h_s, \chi)$ is the boundary mapping matrix from the genetic basis to the kinematic data at the segment ends; and $ds_s^{(q)}$ is the vector of these boundary data.

Here

$$\mathbf{d}_s^{(q)} = \begin{pmatrix} \sigma_s(0), \sigma_s'^{(0)}, \dots, \sigma_s^{(q)}(0), \\ \sigma_s(h_s), \sigma_s'(h_s), \dots, \sigma_s^{(q)}(h_s) \end{pmatrix}^T. \qquad (19)$$

In (19), σ_s^r denotes the r-th derivative of the segment solution with respect to strain ε; the superscript T denotes transposition. The vector $ds_s^{(q)}$ contains the values of σ_s and its derivatives up to order q at the left end x = 0 and the right end x = h_s of the segment.

For each pair of derivatives, introduce the matrix of genetic integrals

$$\mathbf{G}_{ij}^{(q,s)} = \left[\int_0^{h_s} g_\alpha^{(q)(i)}(x)\, g_\beta^{(q)(j)}(x)\, dx\right]_{\alpha\beta}. \qquad (20)$$

In (20), i and j are the derivative orders entering the

reversible quadratic form, $1 \le i,j \le q+1$; $\alpha,\beta = 1,\ldots,n_q$ number the rows and columns of the matrix $G_{ij}^{(q,s)}$. Each matrix element is the integral of the product of the i-th and j-th derivatives of the corresponding genes over segment s.

Then

$$I_{ij}^{(s)} = \mathbf{f}_s^T \mathbf{G}_{ij}^{(q,s)} \mathbf{f}_s = \mathbf{d}_s^T \mathbf{C}_s^{-T} \mathbf{G}_{ij}^{(q,s)} \mathbf{C}_s^{-1} \mathbf{d}_s. \quad (21)$$

Here $I_{ij}^{(s)}$ is the segment derivative integral introduced in (10); C_s is shorthand for $C^{(q)}(h_s, \chi)$, and $C_s^{-T} = (C_s^{-1})^T$.

Denoting

$$\mathbf{K}_{ij}^{(q,s)} = \mathbf{C}_s^{-T} \mathbf{G}_{ij}^{(q,s)} \mathbf{C}_s^{-1}, \quad (22)$$

The matrix $K_{ij}^{(q,s)}$ in (22) is the matrix of the genetic integral $G_{ij}^{(q,s)}$ reduced to the boundary kinematic data. Therefore, (23) expresses $I_{ij}^{(s)}$ directly in terms of the boundary-data vector d_s.

We obtain

$$I_{ij}^{(s)} = \mathbf{d}_s^T \mathbf{K}_{ij}^{(q,s)} \mathbf{d}_s. \quad (23)$$

Thus, the physical regularizer is evaluated analytically from the passport coordinates and the boundary kinematics of the segments. This fundamentally distinguishes the present work from empirical smoothing: the regularization coefficients are not assigned externally but are physical characteristics of the material and constitute its physical passport.

The segment phenotype is represented in the genetic basis by (17), with boundary closure (18)-(19); the genetic integral matrix (20) gives the derivative integral (21), and its boundary reduction (22) yields the quadratic form (23).

The computational implementation uses a unified exponential genetic basis consistent with the characteristic roots of the operator: C^0, $\{1, \mathrm{x}\}$; for C^1, $\{1, \mathrm{x}, \exp(\lambda_1 \mathrm{x}), \exp(\lambda_2 \mathrm{x})\}$; and for C^2, $\{1, \mathrm{x}, \exp(\lambda_1 \mathrm{x}), \exp(\lambda_2 \mathrm{x}), \exp(\lambda_3 \mathrm{x}), \exp(\lambda_4 \mathrm{x})\}$. The characteristic roots are determined by the identified genes and are common to the segments of the corresponding physical class; the segment index belongs only to the phenotype coefficients. This choice makes the analytical evaluation of derivatives and segment matrices consistent with the operator representation of the Material Passport.

5. Architecture as a Variable: Finite Search and Stopping Condition

Removing the assumption of fixed architecture means that the object of the search is no longer an architecture alone or a physical passport alone, but their joint state. It is convenient to regard the pair "architecture-physics" as a single element of the recognition space

$$X = (\Gamma, \chi), \qquad J(X) = J(\Gamma, \chi). \quad (24)$$

Here Γ specifies the segment boundaries and the sequence of their classes, whereas χ denotes the observable coordinates of the physical passport. These two parts of the state are interdependent: changing a boundary or a class changes the boundary kinematics of the segments and hence the result of the first physical inverse problem; changing the passport, in turn, changes the physical part of the generalized Reinsch functional and may change the preferred architecture. Therefore, the optimal "architecture-physics" structure must be constructed as a sequence of self-consistent states in which the physical passport is reidentified after every architectural change.

This reidentification is an inner fixed-architecture first inverse problem and must not be interpreted as variation of the complete physical passport for the purpose of architectural optimization. Only the observable passport is closed for each candidate before the profiled state is returned to the outer Recognition level.

The experimental sample is finite, but finiteness alone does not require exhaustive enumeration of all

possible one-point partitions. In the present work, the direction of architectural reproduction is determined geometrically by the point of maximum absolute error of the current synthesized phenotype. Only this geometric reproduction operation is inherited unchanged from [12]. Thus, Geometry Builder answers the question "where to reproduce", whereas the Ritz-Reinsch target form answers "what classes should the offspring have" and "how should the local physical alternative be ranked".

Let a fully closed state $X_r = (\Gamma_r, \chi_r*)$ and the set K_r of experimental points not yet used as boundaries be available at step r. For each such point, the absolute defect of the current phenotype is evaluated:

$$e_r(k) = \left| \sigma_k - \widehat{\sigma_r}(\varepsilon_k) \right|, k \in K_r \quad (25)$$

At the next step, only one geometric reproduction operator is considered.

The reproduction point is selected uniquely as the maximum absolute defect among the points not yet used:

$$k_r* = arg\ max_{k \in K_r} e_r(k). \quad (26)$$

The parent segment containing k_r* is split only at this point. All other architecture boundaries are retained:

$$\Gamma_{r+1} = Split(\Gamma_r, k_r^*). \quad (27)$$

After the split, only the classes of the two new offspring segments are varied. The classes of all unchanged segments are inherited from Γ_r. The set of admissible local class pairs is determined by information sufficiency and by the existence of a single phenotype consistent with the contact and boundary conditions:

$$Q_r^{adm} \subseteq \{C^0, C^1, C^2\} \times \{C^0, C^1, C^2\}, \left| Q_r^{adm} \right| \leq 9. \quad (28)$$

For each admissible pair (q_L, q_R), the internal first inverse problem is solved: the roots are fixed by the identified genes, whereas the active g-coordinates are determined from stationarity of the target Ritz-Reinsch 1-form. This defines the fully relaxed observable passport:

$$\lambda_\Gamma = \Lambda(G_{\Gamma_{r+1}}), R_{\Gamma_{r+1}}^{(g)}(\lambda_\Gamma, g_\Gamma) = 0. \quad (29)$$

Among no more than nine local class alternatives, the physically admissible offspring pair with the smallest profiled value of the observable form is selected:

$$(qL*, qR*) = arg\ min_{(qL,qR) \in Q_r^{adm}} JR(\Gamma_{r+1}, \chi * \Gamma_{r+1}). \quad (30)$$

The increment of the target form along the selected geometric direction of maximum defect is evaluated after local class relaxation:

$$\Delta J_r = \hat{J}_R(\Gamma_{r+1}, \chi_{\Gamma_{r+1}}^*) - \hat{J}_R(\Gamma_r, \chi_{\Gamma_r}^*). \quad (31)$$

After the point of maximum absolute defect has been selected, the target Ritz-Reinsch form is used to choose the best physically admissible pair of classes for the two offspring. The sign of an individual increment of J_R is not used as an independent premature stopping criterion while the synthesized phenotype remains experimentally distinguishable at the adopted resolution δ.

Experimental sufficiency of the current state is determined simultaneously by the normalized root-mean-square and maximum errors:

$$E_RMS \leq \delta \ \wedge \ E_\infty \leq \delta \quad (32)$$

As long as at least one of the errors exceeds δ, reproduction continues at the point of the global maximum absolute defect, while J_R ranks the admissible local offspring-class pairs. The trajectory terminates when $E_{RMS} \leq \delta$ and $E_\infty \leq \delta$ hold simultaneously, or when no information-admissible continuation exists at the selected point. For normalized samples in the computational experiment with N data points equally spaced in strain, the unified measure of experimental resolution is $\delta = \frac{1}{N-1}$

$$\delta = 1/(N-1) \quad (33)$$

Consequently, the state obtained is terminal with respect to the selected operator "maximum absolute defect → local relaxation of offspring classes". When $E_{RMS} \leq \delta$ and $E_\infty \leq \delta$ are reached, it is the first experimentally admissible state of this deterministic genealogy and therefore the least complex among its admissible predecessors. This statement does not imply a global minimum over arbitrary alternative partitions.

Finiteness of the procedure follows directly. Introduce an integer-valued rank function equal to the number of experimental reproduction points not yet used,

$$\nu(X_r) = |\mathcal{K}_r|. \quad (34)$$

At every accepted reproduction, the unique point k_r^* becomes an internal boundary and is removed from K_r. Therefore,

$$\nu(X_{r+1}) < \nu(X_r). \quad (35)$$

The rank (34) is a nonnegative integer and strictly decreases at every accepted step. Hence, an infinite sequence of accepted reproductions is impossible: after finitely many steps, either K_r is exhausted or stopping condition (33) is satisfied earlier. If initially there are N_c admissible internal points, the number of accepted splits satisfies the estimate

$$r_{\max} \leq N_c. \quad (36)$$

Thus, finiteness of the sample guarantees finiteness of the deterministic search trajectory. Unlike exhaustive enumeration, criterion (33) applies only to the direction of the maximum absolute defect of the current phenotype. This is a deliberate separation of roles: Geometry Builder determines the reproduction location from the error geometry, Material Builder performs the internal physical closure, and Recognition uses the observable Ritz-Reinsch form to rank the admissible local physical alternatives.

The resulting construction provides a sequential determination of optimal complexity along the maximum-error trajectory: max |e| determines where reproduction occurs; minimization of J_R over no more than nine admissible local class pairs determines what the offspring should be; and attainment of the experimental resolution δ determines when increasing complexity should stop. No external limit on the number of segments or artificial complexity penalty is required.

The recognition state (24) generates the defect field (25), the unique reproduction point (26), and the inherited-boundary update (27). Information-admissible offspring classes are restricted by (28), physically closed by (29), and ranked by (30), with the target-form increment recorded in (31). Experimental sufficiency is measured by (32) and stopped by (33), while the rank (34), its strict decrement (35), and the split bound (36) establish finite termination.

Contact between adjacent segments is imposed kinematically. At an internal boundary, the maximum mandatory order of continuity is determined by the lower of the two adjacent classes. The value σ is always continuous. If the lower class is C^0, no derivative continuity is additionally required. If the lower class is C^1, the additional derivative level is σ', so the contact conditions are σ, σ'. Only a $C^2 - C^2$ contact reaches the second-derivative level σ'', with conditions $\sigma, \sigma', \sigma''$. Thus, a mixed $C^0 - C^1$ contact is governed by the lower class, whereas a mixed $C^1 - C^2$ contact is governed by class C^1. These are kinematic conditions; no additional continuity of variational forces is imposed across an internal boundary.

The external boundary conditions are likewise class-dependent. At each external boundary, only the boundary operator corresponding to the class of the end segment is used. Therefore, the natural coordinates g_0 and g_1 of the highest class C^2 are activated only when the corresponding left or right external boundary belongs to a C^2 segment. If the end segment has class C^0 or C^1, C^2 conditions are not transferred to it, and inactive passport coordinates are excluded from the observable projection rather than set equal to zero.

6. Irreversible Processes: From Stationarity of the Pfaffian Form to a Finite-Dimensional Reinsch Target Function

For an irreversible material, the tensor of physical properties is represented as

$$C_{ij} = A_{ij} + B_{ij}, \quad A_{ij} = A_{ji}, \quad B_{ij} = -B_{ji}. \quad (37)$$

The symmetric part A defines the reversible quadratic form. The antisymmetric part B has a fundamentally different mathematical and physical meaning. Antisymmetry implies

$$\sum_{i,j} B_{ij}\, \sigma^{(i)} \sigma^{(j)} = 0, \quad (38)$$

and therefore it cannot be represented as an additional potential energy. Its primary objects remain the nonintegrable antisymmetric Pfaffian 1-forms introduced in (7).

This is precisely where the proposed approach differs fundamentally from the Ritz method. In the classical Ritz method [14], a finite-dimensional approximation is substituted into a potential-energy functional, after which stationarity of the potential energy with respect to the approximation amplitudes is required. In the present work, the initial condition is more general: stationarity of a nonintegrable variational Pfaffian form is required. The reversible potential part is only the symmetric component of this formulation, whereas the antisymmetric part describes the work of dissipative forces and, in general, cannot be reduced to the variation of a scalar potential. Therefore, the finite-dimensional form derived below is analogous to the Ritz method in the manner in which the continuous problem is reduced to an algebraic one, but not in the underlying stationarity condition. This distinction is one of the principal results of the present work.

In the variational formulation, the irreversible part for a segment of class C^q is written as

$$\delta W_{B,s}^{(q)} = \int_{\varepsilon_{s-1}}^{\varepsilon_s} \sum_{1\le i<j\le q+1} B_{ij}^{(q)} \left[\sigma_s^{(i)}\,\delta\sigma_s^{(j)} - \sigma_s^{(j)}\,\delta\sigma_s^{(i)}\right] d\varepsilon. \tag{39}$$

In (39), the symbol δ denotes a virtual variation. It must not be identified with the total differential along the actually realized process. After the variational problem has been solved, the accumulated work of the dissipative forces is determined along the actual path of plastic deformation. The elementary Pfaffian channel has the form

$$dD_{ij,s} = B_{ij}^{(q)} \left[\sigma_s^{(i)}\,d\sigma_s^{(j)} - \sigma_s^{(j)}\,d\sigma_s^{(i)}\right], \quad i<j. \tag{40}$$

Here d denotes the total differential along the actual trajectory. The accumulated work of the corresponding dissipative channel is the line integral

$$D_{ij,s} = \int_{\gamma_s} d\,D_{ij,s}, \tag{41}$$

and the total accumulated work of the dissipative forces on the segment is

$$D_{B,s}^{(q)} = \sum_{1\le i<j\le q+1} D_{ij,s}. \tag{42}$$

The experimental trajectory is parameterized by strain ε. Therefore, integration in (41) is performed over the actual strain interval $[\varepsilon_{s-1}, \varepsilon_s]$. Unlike the reversible part, the integral of a Pfaffian form depends on the path, while retaining additivity when the path is partitioned into successive segments.

To obtain a finite-dimensional form analogous to the Ritz method, we use the genetic representation adopted in Section 4,

$$\sigma_s(\varepsilon) = \sum_{\alpha=1}^{n_q} f_{s\alpha}\, g_\alpha^{(q)}(\varepsilon;\chi). \tag{43}$$

Hence,

$$\sigma_s^{(i)} = \sum_{\alpha=1}^{n_q} f_{s\alpha}\, g_\alpha^{(q)(i)}, \tag{44}$$

and, because the phenotype coefficients $f_{s\alpha}$ are constant within a given segment,

$$d\sigma_s^{(j)} = \sum_{\beta=1}^{n_q} f_{s\beta}\; dg_\beta^{(q)(j)}. \tag{45}$$

When the path is parameterized by strain,

$$dg_\beta^{(q)(j)} = g_\beta^{(q)(j+1)} d\varepsilon. \tag{46}$$

Direct substitution of (43)-(46) into the original Pfaffian form (40) gives

$$D_{ij,s} = B_{ij}^{(q)} \sum_{\alpha,\beta=1}^{n_q} f_{s\alpha} f_{s\beta} \int_{\varepsilon_{s-1}}^{\varepsilon_s} \left[g_\alpha^{(q)(i)} g_\beta^{(q)(j+1)} - g_\alpha^{(q)(j)} g_\beta^{(q)(i+1)}\right] d\varepsilon. \tag{47}$$

All integration with respect to strain can now be carried out analytically once, when the segment matrices are constructed. Define the matrix of the

integrated dissipative channel

$$\mathbf{D}_{ij}^{(q,s)} = \left[\int_{\varepsilon_{s-1}}^{\varepsilon_s} \left(g_\alpha^{(q)(i)} g_\beta^{(q)(j+1)} - g_\alpha^{(q)(j)} g_\beta^{(q)(i+1)}\right) d\varepsilon\right]_{\alpha\beta}. \tag{48}$$

Then the accumulated work of a single channel no longer contains an integral over strain:

$$D_{ij,s} = B_{ij}^{(q)} \mathbf{f}_s^T \mathbf{D}_{ij}^{(q,s)} \mathbf{f}_s. \tag{49}$$

Consequently,

$$D_{B,s}^{(q)} = \sum_{1\le i<j\le q+1} B_{ij}^{(q)}\, \mathbf{f}_s^T \mathbf{D}_{ij}^{(q,s)} \mathbf{f}_s. \tag{50}$$

For C^0 there are no independent antisymmetric channels and $D_{B,s}^{(0)} = 0$. For C^1 there is one channel B_{12}, whereas for C^2 there are three channels B_{12}, B_{13}, and B_{23}. Thus, the conventional Pfaffian channels (7) are not replaced by new entities: the matrices $\mathbf{D}_{12}$, $\mathbf{D}_{13}$, and $\mathbf{D}_{23}$ are the result of their already completed integration with respect to strain in the genetic basis.

As in the reversible part, the phenotype coefficients can be eliminated through the boundary kinematics. From (18),

$$\mathbf{f}_s = \mathbf{C}_s^{-1} \mathbf{d}_s. \tag{51}$$

Introduce the reduced matrix of the dissipative channel,

$$\mathbf{L}_{ij}^{(q,s)} = \mathbf{C}_s^{-T} \mathbf{D}_{ij}^{(q,s)} \mathbf{C}_s^{-1}. \tag{52}$$

Then

$$D_{ij,s} = B_{ij}^{(q)} \mathbf{d}_s^T \mathbf{L}_{ij}^{(q,s)} \mathbf{d}_s, \tag{53}$$

and the accumulated work of the dissipative forces of a segment takes the fully integrated form

$$D_{B,s}^{(q)} = \sum_{1\le i<j\le q+1} B_{ij}^{(q)}\, \mathbf{d}_s^T \mathbf{L}_{ij}^{(q,s)} \mathbf{d}_s. \tag{54}$$

For the reversible part, the analogous reduction was already obtained in Section 4. With (22)-(23), its segment contribution can be written as

$$\Pi_{A,s}^{(q)} = \frac{1}{2} \sum_{i,j=1}^{q+1} A_{ij}^{(q)}\, \mathbf{d}_s^T \mathbf{K}_{ij}^{(q,s)} \mathbf{d}_s. \tag{55}$$

Therefore, after analytical integration of relation (7) with respect to strain, the complete physical contribution of each segment becomes a finite-dimensional algebraic form. The integrated target function of the generalized Reinsch principle is

$$\begin{aligned} &J_R(\Gamma, \chi) \\ &= J_D(\Gamma, \chi) \\ &+ \sum_{s=1}^{m} \left[\frac{1}{2} \sum_{i,j=1}^{q_s+1} A_{ij}^{(q_s)}\, \mathbf{d}_s^T \mathbf{K}_{ij}^{(q_s,s)} \mathbf{d}_s \right. \\ &\left. + \sum_{1\le i<j\le q_s+1} B_{ij}^{(q_s)}\, \mathbf{d}_s^T \mathbf{L}_{ij}^{(q_s,s)} \mathbf{d}_s \right]. \end{aligned} \tag{56}$$

In (56), no integrals over strain remain: they have been evaluated analytically and are contained in the matrices $\mathbf{K}_{ij}^{(q,s)}$ and $\mathbf{L}_{ij}^{(q,s)}$. This is the required finite-dimensional analogue of the Ritz reduction.

For an even more compact notation, introduce the effective segment matrix

$$\begin{aligned} \mathbf{H}_s(\chi) = &\frac{1}{2} \sum_{i,j=1}^{q_s+1} A_{ij}^{(q_s)}\, \mathbf{K}_{ij}^{(q_s,s)} \\ &+ \sum_{1\le i<j\le q_s+1} B_{ij}^{(q_s)}\, \mathbf{L}_{ij}^{(q_s,s)}. \end{aligned} \tag{57}$$

Then the target function takes a Ritz-like form,

$$J_R(\Gamma, \chi) = J_D(\Gamma, \chi) + \sum_{s=1}^{m} \mathbf{d}_s^T\, \mathbf{H}_s(\chi) \mathbf{d}_s. \tag{58}$$

Proposition 1 (finite-dimensional reduction of the generalized Reinsch principle). After the segment solution has been represented in a finite genetic basis and the reversible quadratic form and irreversible Pfaffian channels have been integrated analytically, the generalized Reinsch target function is reduced exactly to the finite-dimensional form (56), or equivalently (58), in the boundary kinematic variables of the segments.

Proof. Substitution of the gene expansion (43) into the reversible part yields the G and K matrices of Section 4, whereas substitution of the same expansion

into each antisymmetric channel (40) yields the integrated D and L matrices according to (48) and (52). Since the phenotype coefficients are eliminated by (51), every segment contribution becomes a quadratic form in the boundary-data vector d_s. Summation over all segments gives (56), and grouping the reversible and irreversible matrices gives (57)-(58). No numerical quadrature over strain remains.

The similarity of (58) to the Ritz method is structural: after a finite basis has been selected and the integrals evaluated analytically, the continuous problem is reduced to a finite-dimensional algebraic form. The stationarity principle, however, is different. In the Ritz method, the scalar potential-energy functional is stationary. Here the initial object is the nonintegrable variational 1-form (7); Equation (58) is its integrated finite-dimensional representation along the actual strain path and does not replace Pfaffian stationarity by a potential principle.

The accumulated work of the dissipative forces along the entire segmented trajectory is additive,

$$D_B(\Gamma,\chi)=\sum_{s=1}^{m} D_{B,s}^{(q_s)}, \tag{59}$$

but in general depends on the path traversed. Antisymmetry $B_{ij}=-B_{ji}$ alone does not ensure non-negativity of D_B; here passivity means non-negative accumulated dissipative work along every admissible loading path, and, if required, it must be imposed as a physical constraint on the admissible Material Passport.

For irreversible behavior, the tensor decomposition (37) and antisymmetry condition (38) lead to the variational dissipative form (39). The elementary Pfaffian channel, its path integral, and the total dissipative work are given by (40)-(42); genetic substitutions (43)-(47) convert these objects to the integrated channel matrix (48) and finite forms (49)-(50). Boundary elimination (51), the reduced dissipative matrix (52), and relations (53)-(54) complete the irreversible reduction. Together with the reversible contribution (55), they produce the full target form (56), its effective segment matrix (57), and the Ritz-like representation (58), while (59) records additivity along the segmented trajectory.

Finally, computational use of (56) or (58) is admissible only through genuinely identifiable passport coordinates. Underdetermined components A_{ij} and B_{ij} must not be assigned artificial values merely to close the target function. The relationship between the observable operator and complete physical levels of the Material Passport is considered in the next section.

7. The First Inverse Problem and the Two-Level Material Passport

The present work remains a first inverse identification problem. It must not be allowed to turn implicitly into a second inverse problem or into an underdetermined component-wise reconstruction of all elements of A and B. The natural output object is a unified Material Passport containing two related but distinct subsets.

Accordingly, Recognition compares architectures only after closure of their observable passport. Underdetermined coordinates of the complete physical A/B passport are never introduced as free variables of the architectural search; varying such coordinates independently for architectural identification would constitute a different inverse problem.

The first subset is the observable operator passport of the first inverse problem:

$$P_I^{\mathrm{obs}}=\{\lambda_1,\lambda_2,\lambda_3,\lambda_4,g_0,g_1\}. \tag{60}$$

Here λ_1, …, λ_4 are the characteristic roots of the highest class. They are not free coordinates of an internal minimization: the roots are determined by the identified genes, i.e., by the spectrum of the characteristic operator. The coefficients of the normalized characteristic polynomial follow uniquely from these roots through Vieta relations (63)-(66). The coordinates g_0 and g_1 have a different nature: they are observable combinations of the natural boundary conditions, and their values are determined from stationarity of the target Ritz-Reinsch 1-form on the

actual external C^2 segments. For lower classes, the corresponding nested subset of spectral coordinates is used. Therefore, the active passport projection of a particular architecture χ_Γ consists of the spectral part specified by the genes and only those boundary coordinates that are actually observable for the actual classes of the external segments.

The second subset is the complete physical passport:

$$P_{II}^{A/B} = \{A_{11}, A_{12}, A_{13}, A_{22}, A_{23}, A_{33}; B_{12}, B_{13}, B_{23}\}. \quad (61)$$

These nine components are not declared to be directly measured by the first inverse problem. The relationship between the two levels is specified by the coefficients of the characteristic polynomial and Vieta's theorem. For the normalized characteristic equation

$$p(\lambda) = \lambda^4 + a_3\lambda^3 + a_2\lambda^2 + a_1\lambda + a_0 \quad (62)$$

We have

$$a_3 = -\sum_{r=1}^{4} \lambda_r, \quad (63)$$

$$a_2 = \sum_{i<j} \lambda_i \lambda_j, \quad (64)$$

$$a_1 = -\sum_{i<j<k} \lambda_i \lambda_j \lambda_k, \quad (65)$$

$$a_0 = \prod_{r=1}^{4} \lambda_r. \quad (66)$$

For the normalization adopted in [13], these coefficients are related to the tensor ratios by

$$a_3 = \frac{2B_{23}}{A_{33}}, \quad a_2 = \frac{2A_{13} - A_{22}}{A_{33}}, \quad (67)$$

$$a_1 = -\frac{2B_{12}}{A_{33}}, \qquad a_0 = \frac{A_{11}}{A_{33}}, \quad (68)$$

and the natural boundary conditions provide two further combinations,

$$g_0 = \frac{A_{12} + B_{12}}{A_{33}}, \qquad g_1 = \frac{A_{23} + B_{23}}{A_{33}}. \quad (69)$$

Thus, P_I^{obs} is the directly identifiable level, whereas $P_{II}^{A/B}$ is the physical level of the passport, reconstructed only to the extent that the system of relations has sufficient rank and is supplemented by the required normalization or independent information. Underdetermined components must remain underdetermined rather than being replaced by zeros or artificial values.

The observable operator passport is specified by (60), whereas the complete physical passport is recorded separately in (61). The normalized characteristic Equation (62) is linked to its roots by the Vieta relations (63)-(66); the tensor-ratio relations (67)-(68) and the natural-boundary combinations (69) then connect the observable and complete passport levels to the extent permitted by identifiability.

8. Computational Implementation: Recognition

The computational implementation of the present work is regarded not as a single monolithic program but as a Platform in which separate modules have different responsibilities and exchange strictly defined data objects. The Platform is represented by the tuple

$$\mathcal{P} = (\mathcal{B}_D, \mathcal{G}, \mathcal{M}, \mathcal{R}, \mathcal{U}, \mathcal{Q}). \quad (70)$$

Here $\mathcal{B}_D$ is the bank of experimental datasets; $\mathcal{G}$ is Geometry Builder; $\mathcal{M}$ is Material Builder; $\mathcal{R}$ is the Recognition supervisory layer; $\mathcal{U}$ is the object-oriented user interface; and $\mathcal{Q}$ is postprocessing and result export. This separation is essential: each module solves only its own task and must not implicitly alter the results of another module.

The dataset bank $\mathcal{B}_D$ is the input layer of the Platform. It stores the original discrete relations $\{(\varepsilon_k, \sigma_k)\}_{k=1}^{N}$ and the associated service information required for reproducible computation. The dataset is passed to the computational modules without changing its experimental values. Thus, the source data remain separate from all subsequent geometric and physical interpretations.

Geometry Builder is responsible for the structural part of a step. From the current synthesized phenotype it computes the absolute error at all as-yet unused experimental points and selects the unique reproduction point at the global maximum of that error.

This boundary-location rule, together with retention of all previously accepted boundaries, is the part inherited from [12]. The offspring classes are not assigned by Geometry Builder in the Recognition cycle; they are generated as local admissible alternatives by Recognition and are physically compared only after fixed-architecture closure by Material Builder. After splitting the parent segment, Geometry Builder passes the resulting candidate architecture to Material Builder:

$$D \overset{\mathcal{G}}{\to} \Gamma \overset{\mathcal{M}}{\to} \chi. \tag{71}$$

Material Builder receives the architecture as a fixed input and is not allowed independently to move boundaries or change a segment class. On this architecture it solves the internal first inverse problem in two conceptually distinct stages. First, the characteristic roots are identified from the gene operator, thereby fixing the spectral part of the observable passport. Then, for a single contact-consistent phenotype, only the active natural boundary coordinates g_0 and/or g_1 are determined from stationarity of the target Ritz-Reinsch 1-form. After this, the gauge-invariant observable form $\hat{J}_R$ is evaluated. The complete component-wise A/B passport is not reconstructed.

The software decomposition therefore reproduces the mathematical nesting of the problem: Recognition generates an architectural candidate, Material Builder closes its observable passport at fixed architecture, and only the resulting profiled state is returned to Recognition for comparison.

The Recognition supervisory layer couples Geometry Builder and Material Builder into a single cycle. After the unique geometric split at the point of maximum absolute defect, it considers only admissible classes of the two new offspring segments—no more than nine C^0 / C^1 / C^2 pairs. For each pair, existence of a single class-compatible phenotype is checked; the roots are then fixed by the identified genes, the active g-coordinates are determined by stationarity of the Ritz-Reinsch 1-form, and the profiled value J_R is evaluated. The best admissible pair is selected by J_R, while continuation of the trajectory is determined by the experimental distinguishability of the current phenotype.

$$\begin{aligned} k_{\mathrm{r}} * = arg\ max_{k \in K_{\mathrm{r}}} \left| \sigma_{\mathrm{k}} - \hat{\sigma}_{\mathrm{r}}(\varepsilon_{\mathrm{k}}) \right| \\ \to Split(\Gamma_{\mathrm{r}}, k_{\mathrm{r}} *) \\ \to \{(qL, qR)\} adm \to JR. \end{aligned} \tag{72}$$

Thus, the supervisory module no longer enumerates all possible positions of a new boundary. The geometric direction of a step is uniquely prescribed by the maximum absolute error, whereas the physical comparison is restricted to local relaxation of the classes of the two offspring. Unchanged segments inherit their classes and solutions, eliminating the global enumeration of 3^m class sequences. The cycle is repeated until the prescribed experimental resolution δ is reached or admissible continuation is exhausted.

In this part, the Platform performs a function analogous to sequential DoE, but the direction of the next experiment is not enumerated: it is determined by the maximum of the current absolute defect. The discrete local factors are the classes of the two offspring, while the response is the profiled integrated Ritz-Reinsch form. Hence the DoE logic is generalized from a fixed factor space to a locally generated model space.

The object-oriented interface $\mathcal{U}$ is not part of the mathematical core but a supervisory user layer. It forms a problem object containing a reference to the dataset, the settings of the admissible search, the state of the current architecture, and passport data, and transmits commands to the corresponding computational objects. This design makes it possible to replace or test an individual module without changing the mathematical formulation of the entire Platform. The interface must also explicitly distinguish experimental data, computed quantities, and underdetermined passport components; the latter must not be automatically replaced by zeros.

The postprocessor $\mathcal{Q}$ operates only after completion of a computational step or of the entire search. Its task is to form a traceable representation of the result: the final Material Passport, the synthetic curve, quality

indicators, architecture tables, and the computational service log. The transformation of the terminal state can be written as

$$X^* = (\Gamma^*, \chi^*) \xrightarrow{Q} \{P_{\text{Material}}, \hat{\sigma}(\varepsilon), \mathcal{E}, \mathcal{L}\}. \qquad (73)$$

Here $\mathcal{E}$ denotes the set of quantitative quality indicators, and $\mathcal{L}$ is the trace log that makes it possible to reconstruct the sequence of accepted architectural changes and the corresponding solutions of the first inverse problem. In plots, by contrast, the postprocessor deliberately does not display segment numbers or classes so as not to overload the visualization; this information is retained in tabular and passport data.

Thus, the Platform implements not a sequential launch of two independent utilities but a controlled computational loop. Its information flow can be represented as

$$\mathcal{B}_D \to \mathcal{G} \to \mathcal{R}[\mathcal{M}] \to \mathcal{Q}, \qquad \mathcal{U} \leftrightarrow \mathcal{R}. \qquad (74)$$

Square brackets emphasize the repeated invocation of Material Builder from Recognition. In the new scheme, however, it is invoked not for all possible boundary positions, but only for the local class variants of a single split selected by the maximum absolute defect.

In the corrected implementation, class C^0, C^1, or C^2 is determined separately for each segment, but after reproduction only the two new offspring segments are reconsidered. The classes of all other segments are inherited from the accepted state. For each of no more than nine local pairs, before $\hat{J}_R$ is evaluated, the complete system of kinematic constraints is solved: exact values at the architecture nodes, class-dependent contact conditions, and the external boundary block corresponding to the actual end classes. An incompatible pair is rejected as inadmissible and is not penalized inside the target form.

The analytical kernel of reversible and dissipative segment matrices is used as a common computational layer of Material Builder and Recognition. The existence of this kernel, however, does not justify fictitious reconstruction of the complete component-wise A/B passport. Until the observable passport is fully closed, the Platform must distinguish "directly identified by the first inverse problem", "computed from identified quantities", and "remains underdetermined".

After this separation of identification mechanisms, the stopping condition of the mixed problem is formulated along the deterministic reproduction trajectory. The spectral coordinates are fixed by the genes, the active boundary part of the passport is closed by stationarity of the Ritz-Reinsch 1-form, the point of the new split is specified by the maximum absolute defect, and the classes of the two offspring are selected by the minimum profiled $\hat{J}_R$ among the admissible local pairs:

$$\begin{aligned} & k_{\mathrm{r}} *= arg\ max_{\mathrm{k}} |e_{\mathrm{k}}|;\ \lambda\Gamma = \Lambda(G\Gamma);\ R\Gamma(g) \\ & = 0;\ (qL *, qR *) \\ & = arg\ min_Qadm\, J_R;\ E_RMS \le \delta\ \wedge\ E_\infty \\ & \le \delta \end{aligned} \qquad (75)$$

Condition (75) combines four levels of a single step. The first group selects the unique reproduction point from the maximum absolute error. The second fixes the spectral part of the observable passport by the identified genes and determines the active g-coordinates from the stationary natural-boundary components of the Ritz-Reinsch 1-form. The third selects the best admissible pair of offspring classes while all other segment classes remain unchanged. Completion of the trajectory is determined by attainment of the experimental resolution, $E_{RMS} \le \delta$ and $E_\infty \le \delta$. The terminal state therefore belongs to the selected deterministic maximum-defect trajectory and is not the result of exhaustive enumeration of all possible single-point boundaries.

The Platform decomposition (70) assigns distinct roles to its modules. Geometry Builder supplies the architecture update (71), Recognition performs the local supervisory selection (72), and postprocessing maps the terminal state to traceable outputs through (73). Their repeated information flow is summarized by (74), while the mixed recognition condition (75) closes the computational cycle.

9. Computational Scheme for Determining Optimal Complexity

The computational determination of complexity is

constructed as a sequence of fully closed states $X_r = (\Gamma_r, \chi_r^*)$. At each step, Geometry Builder evaluates the absolute defect of the synthesized phenotype at all experimental points not yet used as nodes and selects the unique reproduction point $k_r^* = \underset{k \in \mathcal{K}_r}{arg\,max} |\sigma_k - \hat{\sigma}_r(\varepsilon_k)|$. This rule determines the direction of the discrete variation and contains no external complexity parameter.

After splitting the parent segment, Recognition considers only admissible classes of the two offspring, $C^0/C^1/C^2$. The classes of all other segments are inherited. A local pair is admitted to comparison only if there exists a single phenotype satisfying information sufficiency, exact nodal data, class-dependent contact conditions, and the external boundary conditions corresponding to the actual classes of the end segments.

For each admissible candidate, Material Builder closes the observable projection of the Material Passport $\chi\Gamma$ anew: the characteristic roots are determined by the identified genes, while the active g_0 and g_1 are determined by the stationary natural-boundary components of the target Ritz-Reinsch 1-form. Only after this closure is the profiled gauge-invariant form $\int_R(\Gamma, \chi_\Gamma^*)$ evaluated.

For the selected reproduction point, the profiled $\int_R$ determines the physically preferable admissible pair of offspring classes. As long as $E_{RMS} > \delta$ or $E_\infty > \delta$, this state becomes the next element of the deterministic genealogy and reproduction continues. The first state for which $E_{RMS} \le \delta$ and $E_\infty \le \delta$ simultaneously is accepted as the recognition result at the prescribed resolution δ.

In the terminology of [12], this result should not be called a global optimum, but rather the least-complex experimentally admissible state of the deterministic genealogy. The present work retains from [12] the deterministic geometric reproduction at the maximum defect and preservation of previously accepted boundaries, but supplements this genealogy by a new local physical relaxation of the offspring classes: for each admissible class pair the fixed-architecture physical closure of [13] is performed, after which $\int_R$ selects the physically preferable pair and the observable Material Passport is closed. Accordingly, the term "optimal complexity" is used below only in this restricted sense.

Numerical verification was performed for three reference materials without an external limit on the number of segments. The same sequence was used for every state: the maximum absolute defect determines the reproduction point; the local pair of offspring classes is tested for information and kinematic admissibility; the observable Material Passport is then closed and the profiled form $\int_R$ is evaluated. The results are presented in Fig. 1 and Table 1.

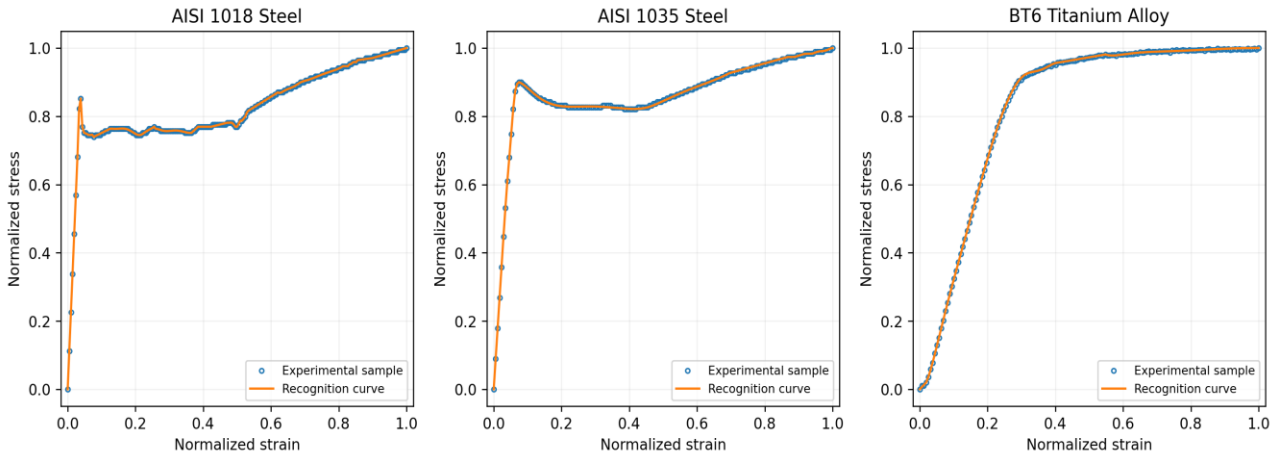


Fig. 1 Experimental datasets and synthesized curves for AISI 1018, AISI 1035, and BT6 obtained along the deterministic trajectory of the maximum absolute defect.

Table 1 Results for AISI 1018, AISI 1035, and BT6 along the deterministic trajectory of the maximum absolute defect. For each dataset, $\delta = \frac{1}{N-1}$; in every case $E_{RMS} \le \delta$ and $E_\infty \le \delta$. The values in parentheses give the total numbers of $C^0/C^1/C^2$ segments, respectively, not their order along the deformation curve.

Material	m ($C^0/C^1/C^2$)	RMSE, normalized	E∞, normalized	δ	Status
AISI 1018 Steel	13 (10/0/3)	0.005039	0.013611	0.016129	admissible
AISI 1035 Steel	10 (5/0/5)	0.002220	0.005535	0.005682	admissible
BT6 Titanium Alloy	5 (2/0/3)	0.002015	0.006265	0.006369	admissible

For AISI 1018, AISI 1035, and BT6, the complete computation proceeded along the deterministic trajectory of the maximum absolute defect until the prescribed experimental resolution was reached. In all three cases, $E_{RMS} \le \delta$ and $E_\infty \le \delta$ were satisfied simultaneously.

The results show that the physical target form and experimental accuracy perform different functions. The maximum absolute defect localizes the next reproduction; J_R selects the physically preferable admissible pair of offspring classes; and the conditions $E_{RMS} \le \delta$ and $E_\infty \le \delta$ determine attainment of the experimental resolution. Thus, complexity is not prescribed in advance but emerges from sequential self-consistent identification of the architecture and the observable passport.

10. Discussion

The principal result of the present work is the transition from the sequential scheme "morphology first, physics second" to a unified variational recognition problem in which the architecture Γ and the physical passport χ are interdependent variables of one target form. The essential novelty of this formulation appears in three successive generalizations.

The first generalization concerns the Ritz method. The similarity lies in the mechanism of finite-dimensional reduction: after a finite basis has been selected, the continuous integrals are evaluated analytically and the problem is reduced to an algebraic form in a finite set of coordinates. The underlying stationarity principle, however, is fundamentally different. The Ritz method requires stationarity of potential energy with respect to approximation amplitudes. In material genetics, the primary object is the nonintegrable variational Pfaffian form (7), which includes both the symmetric reversible and antisymmetric dissipative parts. Therefore, the resulting finite-dimensional expression is a Ritz analogue in the reduction mechanism, but not in the physical nature of the variational principle.

The second generalization concerns the Reinsch principle. In the classical smoothing spline, the compromise between agreement with data and smoothness is controlled by an external parameter. In the present work, the mathematical regularizer is replaced by a physical form determined by the Material Passport: the reversible part is specified by the symmetric tensor A, whereas the accumulated work of dissipative forces is represented by the antisymmetric Pfaffian channels of tensor B. After analytical integration, both parts enter a single finite-dimensional target form together with the data misfit.

The third generalization concerns DoE. In classical design of experiments, the factors and the model class are specified in advance. In Recognition, the direction of the next structural experiment is selected by the current phenotype itself—the point of maximum absolute error; only the classes of the two offspring are then varied, and the observable passport of every admissible variant is closed by the genes and by stationarity of the target 1-form. The resulting composition is explicit: [12] supplies deterministic geometric reproduction, the present work generates the local offspring-class alternatives, and the fixed-architecture physical closure developed in [13] is applied to every admissible alternative before J_R performs the local physical selection. Condition (75) therefore characterizes the terminal state of a sequential variational trajectory rather than the result of an

exhaustive enumeration of all possible architectures.

These three generalizations form a single logical chain: Ritz provides the prototype of finite-dimensional variational reduction; Reinsch couples approximation with regularity; the Pfaffian formulation of material genetics transfers this construction to an irreversible material; and condition (75) couples deterministic reproduction at the maximum defect, physical selection of classes by $\int_R$, and attainment of the prescribed experimental resolution. Recognition therefore implements not a global enumeration of architectures, but a self-consistent construction of the deterministic "architecture-physics" genealogy.

At the same time, the observability principle is preserved. The first inverse problem directly determines the operator level of the Material Passport—the spectral coordinates and the observable combinations of the natural boundary conditions. The complete set of A and B components belongs to the second passport level and can be reconstructed only within the rank of the linking relations. This restriction is especially important for the dissipative part: underdetermined components must not be assigned artificially merely to close a numerical model.

The computational scheme of Section 9 implements condition (75) as a sequential construction of self-consistent states. For a prescribed δ, the result is the first state that simultaneously satisfies $E_{RMS} \le \delta$ and $E_{\infty} \le \delta$, i.e., the least-complex experimentally admissible state of the deterministic Recognition genealogy. It is not a global minimum over the set of all possible partitions.

The identification trilogy thus acquires a complete structure: [12] determines the architecture, [13] identifies the physics of a fixed architecture, and the present work seeks their self-consistent combination through a unified finite-dimensional target form. The resulting Material Passport becomes the terminal state of recognition and a natural initial object for subsequent problems of reflection, mutation, evolution, and directed synthesis in material space.

11. Conclusion

The present work formulates a joint first inverse problem of machine recognition of an elastoplastic material, in which morphology, local segment classes, and the observable physical passport are determined as interrelated variables of a unified variational formulation.

The problem is joint in the sense of iterative self-consistency, but nested in its mathematical solution: architecture is varied only at the outer deterministic Recognition level, whereas the observable passport is closed by the inner fixed-architecture first inverse problem. Variation of underdetermined components of the complete physical passport as independent variables of architectural identification would constitute a different, second inverse problem and is outside the scope of the present work.

The principal theoretical result is the finite-dimensional reduction of the generalized Reinsch principle for an irreversible material. After the solution is represented in the genetic basis, the reversible integrals and antisymmetric Pfaffian channels are analytically integrated with respect to strain and contracted into segment matrices. The target form is thereby written without strain integrals in the form (58). This construction is analogous to the Ritz method in the transition from a continuous to a finite-dimensional problem, but the stationarity principle is the nonintegrable Pfaffian 1-form rather than potential energy.

The second result is a physical generalization of the Reinsch principle. The external mathematical smoothing parameter is replaced by properties of the material itself: the symmetric tensor A determines the reversible part, the antisymmetric tensor B determines the dissipative channels, and their integrated form together with the misfit constitutes the recognition target function.

The third result is the refined mixed condition (75). Geometry Builder specifies the reproduction point by the maximum absolute defect; Recognition examines

no more than nine admissible pairs of offspring classes; the characteristic roots are determined by the genes, the active g_0/g_1 by stationarity of the natural-boundary components of the Ritz-Reinsch 1-form, and the profiled J_R selects the physically preferable local pair of classes. For a prescribed δ, the first state satisfying $E_{RMS} \le \delta$ and $E_\infty \le \delta$ is the least-complex experimentally admissible state of the deterministic genealogy.

Thus, [12] → [13] → the present work forms the identification trilogy "structure → physics → machine recognition". The observable passport is closed as follows: the characteristic roots are specified by the genes, the active boundary combinations by stationarity of the Ritz-Reinsch 1-form, while the complete A/B passport is not required for the first inverse problem. At a prescribed δ, the recognition result is the least-complex experimentally admissible state of the deterministic Recognition genealogy; no global minimum over all possible partitions is claimed.

References

[1] Legendre, A.-M. 1805. *Nouvelles méthodes pour la détermination des orbites des comètes*. Paris: Firmin Didot.

[2] Runge, C. 1901. "Über empirische Funktionen und die Interpolation zwischen äquidistanten Ordinaten." *Zeitschrift für Mathematik und Physik* 46: 224-43.

[3] Sobolev, S. L. 1938. "On a Theorem of Functional Analysis." *Matematicheskii Sbornik* 4 (46) (3): 471-97.

[4] Schoenberg, I. J. 1964. "Spline Functions and the Problem of Graduation." *Proceedings of the National Academy of Sciences of the United States of America* 52 (4): 947-50. doi:10.1073/pnas.52.4.947.

[5] Reinsch, C. H. 1967. "Smoothing by Spline Functions." *Numerische Mathematik* 10 (3): 177-83. doi:10.1007/BF02162161.

[6] Fisher, R. A. 1935. *The Design of Experiments*. Edinburgh: Oliver and Boyd.

[7] Douglas, D. H., and Peucker, T. K. 1973. "Algorithms for the Reduction of the Number of Points Required to Represent a Digitized Line or Its Caricature." *The Canadian Cartographer* 10 (2): 112-22. doi:10.3138/FM57-6770-U75U-7727.

[8] Belov, P. A. 2026. "Foundations of the Genetics of Elastoplastic Materials." *Journal of Civil Engineering and Architecture* 20: 129-46. doi:10.17265/1934-7359/2026.04.001.

[9] Belov, P. A., and Golovina, N. Ya. 2026. "Structural Theory of Elastoplastic Material Models." *Journal of Civil Engineering and Architecture* 20: 281-91. doi:10.17265/1934-7359/2026.07.003.

[10] Belov, P. A., and Weiss, E. 2026. "Direct and First Inverse Problems of Genetic Identification of Materials at a Fixed Smoothness Class." *Journal of Civil Engineering and Architecture* 20: 322-39. doi:10.17265/1934-7359/2026.08.002.

[11] Belov, P. A., and Weiss, E. 2026. "The Second Inverse Problem of Genetic Identification of Materials: Selection of the Optimal Model Architecture." *Journal of Civil Engineering and Architecture* 20: 347-58. doi:10.17265/1934-7359/2026.08.004.

[12] Belov, P. A., Golovina, N. Ya., and Weiss, E. 2026. "Morphology of the Deformation Curve of Elastoplastic Materials." *Journal of Civil Engineering and Architecture* 20: 385-99. doi:10.17265/1934-7359/2026.09.003.

[13] Belov, P. A., Golovina, N. Ya., and Weiss, E. 2026. "Physical Property Passport in the Genetics of Elastoplastic Materials." *Journal of Civil Engineering and Architecture* 20: 400-16. doi:10.17265/1934-7359/2026.09.004.

[14] Ritz, W. 1909. "Über eine neue Methode zur Lösung gewisser Variationsprobleme der mathematischen Physik." *Journal für die reine und angewandte Mathematik* 135: 1-61. doi:10.1515/crll.1909.135.1.